Optimal Chiller Loading in Dual-Temperature Chilled Water Plants for Energy Saving

Lizhi Jia[a,b], Junjie Liu[a,*], Shen Wei[b]

[a]Tianjin Key Laboratory of Indoor Air Environmental Quality Control, School of Environmental Science and Engineering, Tianjin University, Tianjin 300072, P.R. China

[b]The Bartlett School of Construction and Project Management, University College London (UCL), London, WC1E 7HB, United Kingdom

Abstract: Buildings account for almost 40% of global energy consumption. Due to the high energy consumption of chilled water plants, various studies have optimized chiller loading in plants with multiple chillers for energy conservation. However, few studies have optimized dual-temperature chiller plants, even though better energy efficiency could be achieved than that of typical single-temperature chiller plants. This paper proposes two optimal control strategies for dual-temperature chilled water plants, strategy B and strategy C. Strategy B optimizes the cooling load distribution of the chillers in each group by adjusting the cooling load ratio of each chiller. Under this strategy, the energy consumption of the chiller plant for the entire cooling season was reduced by 10.1%. Meanwhile, strategy C optimizes the cooling load distribution among chillers in the same chiller group and between two chiller groups, by

simultaneously adjusting the temperature setpoint of the air leaving the primary cooling coils and the partial load ratio of each chiller. By considering both the impact of the chilled water loop and the air handling process, strategy C achieved greater energy saving (16.4%) for the entire cooling season. In hot summer months, the energy savings arise mainly from optimization of the cooling load distribution among chillers in each chiller group, as this optimization accounts for 63–68% of the total savings. In moderate months, optimizing the cooling load distribution among chillers in the same group and optimizing the distribution between two chiller groups account for nearly the same proportion of the total energy savings.

Keywords: Building energy, Dual-temperature chilled water plant, Optimal control, Optimal chiller loading.

1. Introduction

Buildings account for almost 40% of global energy consumption [1, 2], and reducing the energy demand of buildings has become an essential component of global sustainability [3, 4]. In a building, a large proportion of the energy is consumed by the heating, ventilation, and air conditioning (HVAC) system in providing a comfortable and healthy indoor environment [5, 6]. For space cooling, a central cooling system composed of multiple chillers is a popular solution, and it accounts for 25–50% of the building's energy use [7]. The temperature and humidity independent control (THIC) air-conditioning system

has shown significant energy conservation potential [8]. In THIC systems, the sensible cooling load is removed by medium-temperature chilled water. Humidity removal by the THIC fresh air system is 30-40% higher than by conventional air conditioning systems [8], as the fresh air system processes the whole latent cooling load. Thus, the chilled water temperature must be low enough to process the outdoor air humidity to a relatively low value. In this situation, a dual-temperature chilled water plant is more energy-efficient than a single-temperature plant [9, 10]. This is because a dual-temperature plant uses medium-temperature chillers with high energy efficiency for fresh air pre-cooling. However, the control and operation of a dual-temperature chilled water plant are more complicated than for a single-temperature plant, since the cooling load distribution, both among chillers in each group and between medium- and low-temperature chiller groups, significantly impact system energy consumption.

The control of chillers includes sequencing and loading. The sequencing control determines the number of chillers in operation. Typical sequencing control strategies for chillers are based mainly on the cooling load, chilled water return temperature, bypass flow rate, and power input [11, 12]. Among these methods, the cooling load-based strategy is widely used because other strategies employ indirect cooling load indicators. However, this strategy cannot ensure minimum energy consumption. Huang et al. [13] improved the cooling load-based sequencing control method by adjusting the critical point of chiller staging, as

chiller cooling capacity varies with operating conditions. In addition, Liu et al. [14] improved the method by estimating a chiller's maximum cooling capacity under various weather conditions. To maximize the coefficient of performance (COP) of the system, Ahn et al. [15] developed a COP-based sequencing control strategy that reduced system energy consumption by 20.9%, compared with the chilled water return temperature-based strategy. Li et al. [16] and Liao et al. [17] analyzed the robustness of various sequencing strategies. They proposed a hybrid sequencing control strategy that used the complementarity of different load indicators, achieving greater robustness with a switch number reduction of over 15.6%. Liao and Huang [18] proposed a hybrid predictive sequencing control strategy using cooling load prediction as a corrective measure to reduce unnecessary actions (20.0%) and system energy consumption (6.7%).

Meanwhile, the loading process control allocates the cooling load among chillers to meet the cooling demand. Setting an equal load ratio for all chillers is a simple loading method for chillers with identical capacities [19]. To provide control flexibility, the use of chillers with slightly different cooling capacities has been recommended [20]. With non-identical capacities, chillers can be controlled with equal partial derivatives of their respective energy consumptions [19]. However, this method cannot guarantee minimized power consumption in practice, since chiller performance varies, even among chillers with identical

cooling capacities [19, 21]. To improve system energy efficiency, numerous studies have focused on optimal chiller loading (OCL). Chang et al. [22, 23] employed the Lagrangian method to optimize the chillers' cooling load distribution and minimize system energy consumption. Compared with the conventional equal loading strategy, the optimal loading control method reduced energy consumption by 4.2-6.1% in a plant with identical chillers and 6.1-9.4% with non-identical chillers. Since the Lagrangian method is suitable only for convex function optimization, other approaches have been introduced, including the genetic algorithm (GA) [24, 25], branch and bound [26], simulated annealing [27], and evolution strategy [28]. In recent years, many new metaheuristic optimization algorithms and their variants have been studied, with the aim of improved convergence ability, optimal solution accuracy, and robustness. These algorithms include particle swarm optimization (PSO) [29, 30], the improved firefly algorithm [31], differential cuckoo search [32], improved ripple bee swarm [33], improved invasive weed [34], the exchange market algorithm [35], two-stage differential evolution [36], artificial fish swarm [37], and augmented group search [38]. The algorithms' performance has been verified in commonly used cases initially proposed by Chang et al. [22, 25]. In addition, Askarzadeh and Coelho [39] introduced daily optimal chiller loading (DOCL), in which decision variables in a 24-hour period should be tuned simultaneously to minimize the total energy consumption. Beghi et al. [40, 41] optimized the

control of chiller loading and sequencing simultaneously using a multi-phase GA and PSO. They evaluated this optimization approach on systems with identical or mixed types of chillers. Compared with sequential and symmetric strategies, the approach reduced the seasonal energy demand by 13.81% and 7.05%, respectively, while providing good load profile tracking. Chen et al. [42] integrated the PSO algorithm with an artificial neural network to optimize the cooling load distribution. This method reduced energy consumption by over 12.68% with fast convergence and high accuracy. Chan et al. [43] used the ANN model and the GA to minimize the power consumption of a multiple-type-chiller plant, and this method reduced power consumption by 5.26% to 16.68% over the manual method in different months of the year.

The studies mentioned above, which addressed optimal chiller loading and sequencing control, demonstrated a wide range of energy-saving potential. However, the studies were all focused on single-temperature chiller plants. Few studies have looked at optimal control of dual-temperature chilled water plants. For dual-temperature chiller plants, determining optimal operation is more complicated because of the different performance curves among chillers and a larger number of constraints. The cooling load allocation between medium- and low-temperature chiller groups greatly affects the overall energy performance of the plant. Optimal chiller loading of a single-temperature chiller plant considers the impact of the cooling load distribution among chillers. In

comparison, optimal control of dual-temperature chiller plants must also balance the energy consumption between two chiller groups, and this optimization problem is subject to more constraints. The current study proposed two optimal chiller loading strategies for a dual-temperature chiller plant. The formulations for different optimal control strategies, including decision variables, objective functions, and constraints, were analyzed. Finally, the performance of the proposed optimal control strategies was evaluated in a dual-temperature chilled water plant in a semiconductor factory throughout the entire cooling season, and a detailed analysis was performed on two typical days.

This paper makes several contributions that improve the energy efficiency of chiller plants. First, optimization was proposed for the cooling load distribution in a dual-temperature chiller plant, which is rarely seen in the literature. Second, the proposed optimal control strategy considered the cooling load distribution both among chillers in each chiller group and between two chiller groups, by simultaneously optimizing the cooling loads of the chillers and the temperature of the air leaving the primary cooling coils. Third, the optimization method also considered the impact of operating conditions on the cooling coils' maximum capacity, which limits the upper bound of the cooling supply of the corresponding chiller group.

2. Methodology

2.1 Dual-temperature chilled water plant

This study focused on a dual-temperature chilled water plant serving make-up air units (MAUs). The system consists of two decoupled chiller groups, a medium-temperature group and a low-temperature group, as shown in Figure 1. The medium-temperature chiller group supplies chilled water to primary cooling coils for outdoor air pre-cooling, and the low-temperature chiller group provides cold coolant to secondary cooling coils for further cooling and dehumidification. In each group, multiple chillers are employed. In the chilled water loop, fixed-speed primary pumps maintain a constant water flow rate in the chillers, and variable-speed secondary pumps respond to the cooling load variation. In the cooling water loop, cooling towers exhaust heat from the chillers to the ambient environment.

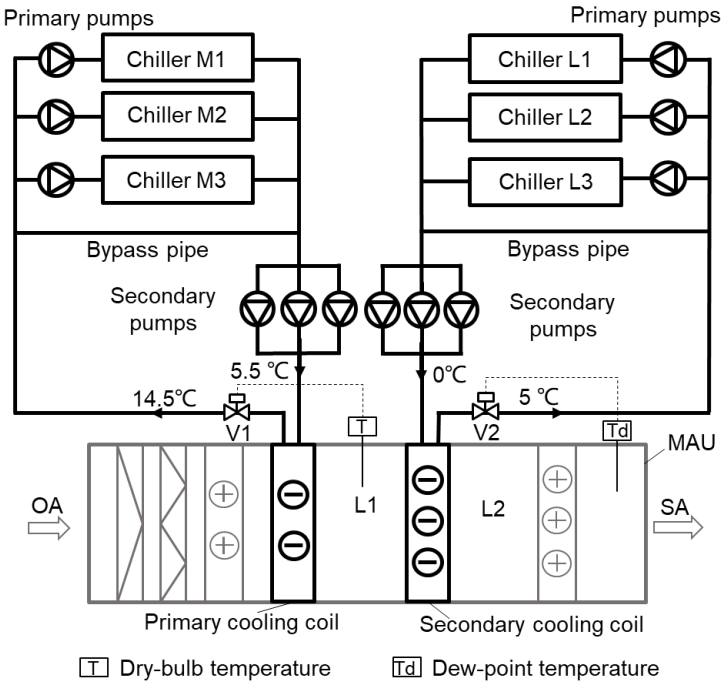

Figure 1: Dual-temperature chilled water plant serving MAUs

The air handling process in the MAUs is shown in Figure 2. In summer, the fresh air is pre-cooled and dehumidified by the primary cooling coils. The air handling process is generally simplified as a straight line between the starting and ending states of the air, OA-L1, as shown in Figure 2. Actually, the air handing process can be divided into two sections: dry cooling, and cooling and dehumidification. When the surface temperature of the cooling coils is lower than the dew-point temperature of the inlet air, the cooling coils operate in a wet state, the air dry-bulb temperature is reduced first with constant humidity, and then the air temperature and humidity are reduced along the saturation curve, as the blue dash line shown in Figure 2. In this situation, the relative humidity of the air leaving the wet cooling coils typically ranges from 90% to 95%. When

the surface temperature of the cooling coils is higher than the dew-point temperature of the inlet air but lower than the dry-bulb temperature of the inlet air, the cooling coils operate in a dry state. Thus, the air dry-bulb temperature is reduced, while the air humidity remains unchanged. After the primary cooling coils, the fresh air is further cooled and dehumidified to the state point of L2.

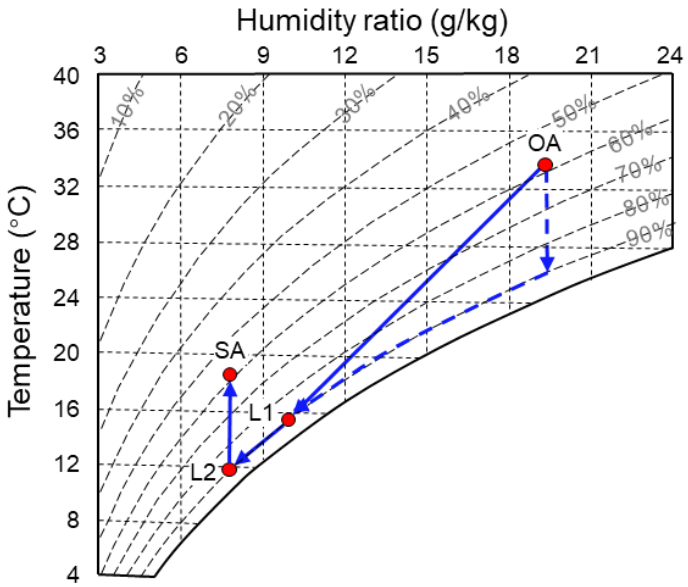

Figure 2. Psychrometric process for fresh air handling during the summer

A dual-temperature chilled water system provides medium-temperature chilled water and low-temperature coolant to the primary and secondary cooling coils, respectively. The flow rate of the medium-temperature chilled water is regulated by adjusting the valve opening of V1 to maintain the outlet air temperature of the primary cooling coils. The flow rate of the low-temperature coolant is adjusted to track the supply air dew-point temperature setpoint (9.5 °C) and then maintain the indoor humidity setpoint (45 ± 5%, 22 ± 1°C). The cooling loads of the primary and secondary cooling coils can be expressed as

Equations (1) and (2):

$$CL_{pri} = M_a(h_{OA} - h_{L1}) \quad (1)$$

$$CL_{sec} = M_a(h_{L1} - h_{L2}) \quad (2)$$

where CL_{pri} and CL_{sec} are the cooling loads of the primary and secondary cooling coils, respectively, kW; M_a is the fresh air mass flow rate, kg/s; and h_{OA}, h_{L1}, and h_{L2} are the air enthalpy at different state points, kJ/kg. The air enthalpy can be calculated from the air temperature and humidity according to Equation (3). As discussed above, in the air handling process, the humidity of the air leaving the primary cooling coils is defined by Equation (4).

$$h = 1.006t + d(2501 + 1.86t) \quad (3)$$

$$\begin{cases} \varphi_{L1} = 90\% & T_{Coil} < T_{dp,OA} \\ d_{L1} = d_{OA} & T_{Coil} \geq T_{dp,OA} \end{cases} \quad (4)$$

where t is the air dry-bulb temperature, °C; d is the moisture content of the air, kg/kg; and φ is the relative humidity of the moist air, %.The moisture content and the relative humidity can be converted from one to the other according to Equation (5),

$$d_{L1} = 0.621945 \frac{\varphi_{L1} p_{w,s}}{p - \varphi_{L1} p_{w,s}} \quad (5)$$

where p and $p_{w,s}$ are the atmospheric pressure and vapor pressure, respectively, of saturated air at t_{L1}, Pa. The vapor saturation pressure for the temperature range of 0 to 200 °C is given by Equation (6) [45],

$$\ln(p_{w,s}) = \frac{C_1}{T} + C_2 + C_3 T + C_4 T^2 + C_5 T^3 + C_6 lnT \quad (6)$$

where $T = t + 273.15$ is the air dry-bulb temperature, K; $C_1 = -5.8002206 \times 10^3$, $C_2 = 1.3914993$, $C_3 = -4.8640239 \times 10^{-2}$, $C_4 = 4.1764768 \times 10^{-5}$, $C_5 = -1.4452093 \times 10^{-8}$, and $C_6 = 6.5459673$.

2.2 Optimization Methodology

2.2.1 Problem formulation

The aim of optimal chiller loading is to determine the cooling load distribution that minimizes the total energy consumption without violating operating constraints. For a dual-temperature chilled water plant, the objective function is the total energy consumption of the chillers, including both the medium- and low-temperature chiller groups, as defined in Equation (7),

$$J = \sum_{i=1}^{N} S_i \times P_i + \sum_{j=1}^{L} S_j \times P_j \quad (7)$$

where S is the state of the ith chiller; P is the power consumption of the ith chiller, kW; N is the total number of medium-temperature chillers, and L is the total number of low-temperature chillers.

The power consumption of a chiller is typically affected by the cooling load, chilled water supply temperature, and cooling water inlet temperature, and it is normally defined by Equation (8) [28],

$$P_{ch,i} = k_{0,i} + k_{1,i}\left(T_{cw,i} - T_{chw,i}\right) + k_{2,i}\left(T_{cw,i} - T_{chw,i}\right)^2 + k_{3,i}Q_i + k_{4,i}\,{Q_i}^2 + k_{5,i}\left(T_{cw,i} - T_{chw,i}\right)Q_i \quad (8)$$

In a typical decoupled chiller plant, the chilled water flow rate in the chillers is

constant. Based on the heat balance, the cooling load of the *i*th chiller is calculated by Equation (9),

$$Q_i = c_p\, m_i\left(T_{chw,r,i} - T_{chw,s,i}\right) \tag{9}$$

As the chilled water return temperatures are identical within the same group, the cooling load of each chiller can be adjusted by regulating the chilled water supply temperature of that chiller. The total cooling load of the system is expressed by Equation (10),

$$CL = c_p\, m_{Total}\left(T_{chw,r} - T_{chw,s}\right) \tag{10}$$

When the cooling load of a chiller is known, Equations (9) and (10) can be used to calculate the chilled water supply temperature of that chiller.

$$T_{chw,s,i} = T_{chw,r} - \frac{Q_i}{F_i CL}\left(T_{chw,r} - T_{chw,s}\right) \tag{11}$$

where F_i is the ratio of the *i*th chiller's mass flow rate to the total; $T_{chw,r}$ is the chilled water return temperature; $T_{chw,s}$ is the total chilled water supply temperature. In this case, the total chilled water temperature ($T_{chw,s}$) varies in a small range, and the most frequent value is 6.3°C; thus, the $T_{chw,r}$ can be obtained by Equation (10) for a given cooling load. As the cooling load and the chilled water supply temperature are non-independent variables, the power consumption model for the chillers was simplified as the function of cooling load and cooling water temperature, and the partial load ratio of the chillers was used to replace the cooling load of each chiller, expressed by Equations (12) and (13).

$$P_i = a_i + b_i PLR_i + c_i T_{cw} + d_i {PLR_i}^2 + e_i PLR_i T_{cw} + f_i {T_{cw}}^2 \quad (12)$$

$$PLR_i = \frac{Q_i}{Q_{rate,i}} \quad (13)$$

where $a_i - f_i$ are coefficients of the ith chiller; T_{cw} is the cooling water temperature. PLR_i is the partial load ratio of the ith chiller; Q_i is the cooling supply of the ith chiller, kW; and $Q_{rate,i}$ is the rated cooling capacity of the ith chiller, kW. The cooling water temperatures (T_{cw}) of all chillers are the same because the sumps of all the cooling towers are connected. The T_{cw} can be obtained from sensors in real applications, and T_{cw} is a known parameter in the optimization.

2.2.2 Constraints

Optimal chiller loading is a constraint optimization problem. The potential optimal control solution is subject to the following operational constraints:

1) Bounds of decision variables

The partial load ratio of the chillers in operation ($S_i = 1$) should be higher than 0.5 because a surge may occur when the cooling load of a chiller drops to 50%. This constraint is defined in Equation (14):

$$\begin{cases} 0.5 \le PLR_i \le 1 & \text{if } S_i = 1 \\ PLR_i = 0 & \text{if } S_i = 0 \end{cases} \quad (14)$$

2) Cooling load balance

In a dual-temperature chilled water plant, the cooling supply by the two chiller groups is required to satisfy the cooling demand of the corresponding cooling coils, as expressed by Equations (15) and (16):

$$\sum_{i=1}^{N} S_i(PLR_i \times Q_{rate,i}) = CL_{pri} \tag{15}$$

$$\sum_{j=1}^{L} S_j(PLR_j \times Q_{rate,j}) = CL_{sec} \tag{16}$$

2.2.3 PSO Algorithm

Optimal chiller loading in a dual-temperature chilled water plant is a multivariable, nonlinear, constrained optimization problem. Metaheuristic optimization algorithms can efficiently solve the optimization of the chiller plant's control and operation, as they use certain tradeoffs between randomization and local search to explore possible solutions on the global scale [44]. PSO and the GA are widely used algorithms in optimal control of central cooling systems. PSO outperforms the GA not only in obtaining the minimum solution, but also in computation efficiency in terms of speed and memory demand [29]. In addition, PSO is easier to implement because it requires a lower number of hyperparameters. Therefore, the PSO algorithm was employed in this study. The updating rule of the algorithm is described by Equations (17) and (18):

$$v_j^{k+1} = \omega v_j^k + \alpha\epsilon_1\left(p_j^k - x_j^k\right) + \beta\epsilon_2\left(g^k - x_j^k\right) \tag{17}$$

$$x_j^{k+1} = x_j^k + v_j^{k+1} \tag{18}$$

where v_j^{k+1} is the velocity of the jth particle in the $k+1$th generation; x_j^{k+1} is the position of the particle; p_j^k is the best position of the ith particle in the kth generation; g^k is the global best position in the kth generation; ω is the inertia weight; α and β are acceleration constants; and ϵ_1 and ϵ_2 are two random

vectors uniformly distributed between 0 and 1.

2.3 Optimal Control Strategies

For a dual-temperature chilled water plant, the control is more complicated than for a single-temperature chiller plant. Both the cooling load distribution among chillers in the same group and the cooling load allocation between the two chiller groups greatly impact the overall energy efficiency of the dual-temperature plant. In this section, two optimal control strategies are proposed for the dual-temperature chiller plant. The conventional control strategy is also described; this strategy is considered the reference method for performance evaluation.

2.3.1 Strategy A: Conventional control strategy

In the conventional control strategy, medium-temperature chillers are regulated to maintain the dry-bulb temperature of the air leaving the primary cooling coil at a constant setpoint, and low-temperature chillers are adjusted to track the supply air dew-point temperature setpoint. The cooling loads of the medium- and low-temperature chiller groups are expressed by Equations (1) and (2), respectively. The number of chillers in operation is then determined according to Equations (19) and (20). Chillers in the same group are loaded with an equal partial load ratio, as defined in Equations (21) and (22):

$$n = ceil(CL_{pri}/Q_{med,rate}) \tag{19}$$

$$l = ceil(CL_{sec}/Q_{low,rate}) \tag{20}$$

$$PLR_{ave,med} = \frac{CL_{pri}}{n \times Q_{med,rate}} \quad (21)$$

$$PLR_{ave,low} = \frac{CL_{sec}}{l \times Q_{low,rate}} \quad (22)$$

where n and l are the numbers of medium-temperature and low-temperature chillers in operation, respectively; $Q_{med,rate}$ and $Q_{low,rate}$ are the rated cooling capacities of the medium- and low-temperature chillers, respectively, kW; and $PLR_{ave,med}$ and $PLR_{ave,low}$ are the average partial load ratio of the chillers in the medium- and low-temperature groups, respectively.

2.3.2 Strategy B: Optimal chiller loading in each group

The cooling load distribution has a significant impact on the energy consumption of the chiller plant. Therefore, optimal chiller loading is crucial for energy saving in chiller plants. For a dual-temperature chilled water plant, the cooling load distribution consists of two parts, the cooling load distribution among chillers in each group and the cooling load allocation between the two chiller groups. Strategy B optimizes the cooling load of the chillers in each group. The cooling loads of the two chiller groups are calculated according to Equations (1) and (2). The enthalpy of the air leaving the cooling coil can be calculated from the air temperature and humidity according to Equations (3) to (6).

In strategy B, the valve V1 on the outlet pipe of the primary cooling coil is adjusted to regulate the water flow rate and also to maintain a constant temperature for the air leaving the primary cooling coils. Similarly, valve V2 is

regulated to maintain the supply air dewpoint temperature. In this optimization problem, two equality constraints (as expressed by Equations (15) and (16)) are considered by adding penalty terms to the objective function. These two penalty terms are each multiplied by a large positive coefficient. Thus, the objective function can be rewritten as Equation (23):

$$J = \sum_{i=1}^{N} S_i \times P_i + K_1 \left| \sum_{i=1}^{N} PLR_i \times Q_{rate,i} - Q_{pri} \right| + \sum_{j=1}^{M} S_j \times P_j + K_2 \left| \sum_{j=1}^{M} PLR_j \times Q_{rate,j} - Q_{sec} \right| \quad (23)$$

where k_1 and k_2 are the penalty factors, which are normally large positive values.

2.3.3 Strategy C: Optimal chiller loading of the whole plant

As mentioned above, in addition to the cooling distribution within each chiller group, the cooling load allocation between the medium- and low-temperature chiller groups has a significant impact on the overall energy consumption. Therefore, we proposed the optimization of the chiller loading of the whole plant by considering both the chilled water loop and the air handling process, referred to as strategy C in the following section. This strategy aims to optimize the cooling load allocation between two chiller groups and the cooling load distribution among chillers in each group simultaneously. According to Equations (1) and (2), the enthalpy of the air leaving the primary cooling coil determines the cooling load distribution between the two chiller groups. Due to

the limited capacities of cooling coils, the leaving air enthalpy is limited to a certain range, as defined by Equation (24). The maximum cooling capacity of a given cooling coil was estimated with the use of a simple cooling coil model proposed by Wang et al. [46], as expressed by Equation (25):

$$h_{L1,min} \leq h_{L1} \leq h_{L1,max} \tag{24}$$

$$Q_{coil} = \frac{\gamma_1 {M_a}^{\lambda}}{1 + \gamma_2 \left(\frac{M_a}{M_w}\right)^{\lambda}} (T_{in,wet} - T_{chw}) \tag{25}$$

where M_w is the chilled water mass flow rate, kg/s; Q_{coil} is the cooling capacity of the cooling coil, kW; $T_{in,wet}$ is the air inlet wet-bulb temperature for the cooling coils, °C; T_{chw} is the chilled water inlet temperature for the cooling coils, °C; and γ_1, γ_2 and λ are coefficients of the cooling coil performance.

With a constant airflow rate, the maximum cooling capacity of a cooling coil can be achieved by supplying a sufficient amount of chilled water. Thus, the maximum cooling capacity with reference to the design value is expressed as Equation (26):

$$\frac{Q_{coil,max}}{Q_{des}} = \frac{T_{in,wet} - T_{chw}}{T_{a,des} - T_{chw,des}} \tag{26}$$

where $Q_{coil,max}$ and Q_{des} are the maximum cooling capacity and the design cooling capacity of the cooling coil, respectively, kW; and $T_{a,des}$ and $T_{chw,des}$ are the air inlet wet-bulb temperature and chilled water inlet temperature, respectively, under the design conditions, °C.

When Equations (1), (2), and (26) are combined, the lower and upper bounds

of the leaving-air enthalpy are derived as Equations (27) and (28):

$$h_{L1,min} = h_{OA} - \frac{h_{a,des} - h_{out,des}}{T_{a,des} - T_{chw,des}}(T_{OA,wet} - T_{chw}) \quad (27)$$

$$h_{L1,max} = h_{L2} + \frac{h_{a,des} - h_{out,des}}{T_{a,des} - T_{chw,des}}(T_{L1,wet} - T_{chw}) \quad (28)$$

where $T_{OA,wet}$ is the wet-bulb temperature of the outdoor air, °C.

As defined in Equation (4), the leaving-air humidity is known for different operating conditions. Therefore, the dry-bulb temperature of the leaving air is taken as the decision variable in the optimization problem because it is a directly controllable variable. Thus, strategy C minimizes the system energy consumption by simultaneously optimizing the partial load ratio of the chillers and the dry-bulb temperature of the air leaving the primary cooling coils. The objective function of this optimization problem is the same as Equation (23). With the exception of the constraints defined in Equations (14) to (16), the limitation on the leaving air enthalpy is also considered in this strategy, as described by Equations (27) and (28).

3. Results

3.1 Case description

The proposed optimal control strategies were evaluated in a dual-temperature chiller plant serving MAUs in a semiconductor factory in Tianjin, China. In this system, the medium-temperature (5.5 °C) chiller group consisted of three chillers with a cooling capacity of 4572 kW (1300 RT), while three chillers with a cooling capacity of 2286 kW (650 RT) were employed in the low-temperature

(0.0 °C) chiller group. This dual-temperature chilled water plant provided cooling for 11 MAUs with a design airflow rate of 80000 m^3/h. The medium-temperature chilled water was regulated to maintain the temperature of the air leaving the primary cooling coils at 15.5 °C. The low-temperature chilled water was adjusted to track the supply air dew-point temperature setpoint of 9.5 °C. Based on historical operation data, the chiller models were established using the regression method. The regression results are shown in Figure 3 and Table 1. The R^2 values of the regression models of the chillers were greater than 0.84, which indicates that the models can predict the changing trend of the chiller energy consumption accurately. Therefore, these models were used to optimize the cooling load of the chillers in the following sections.

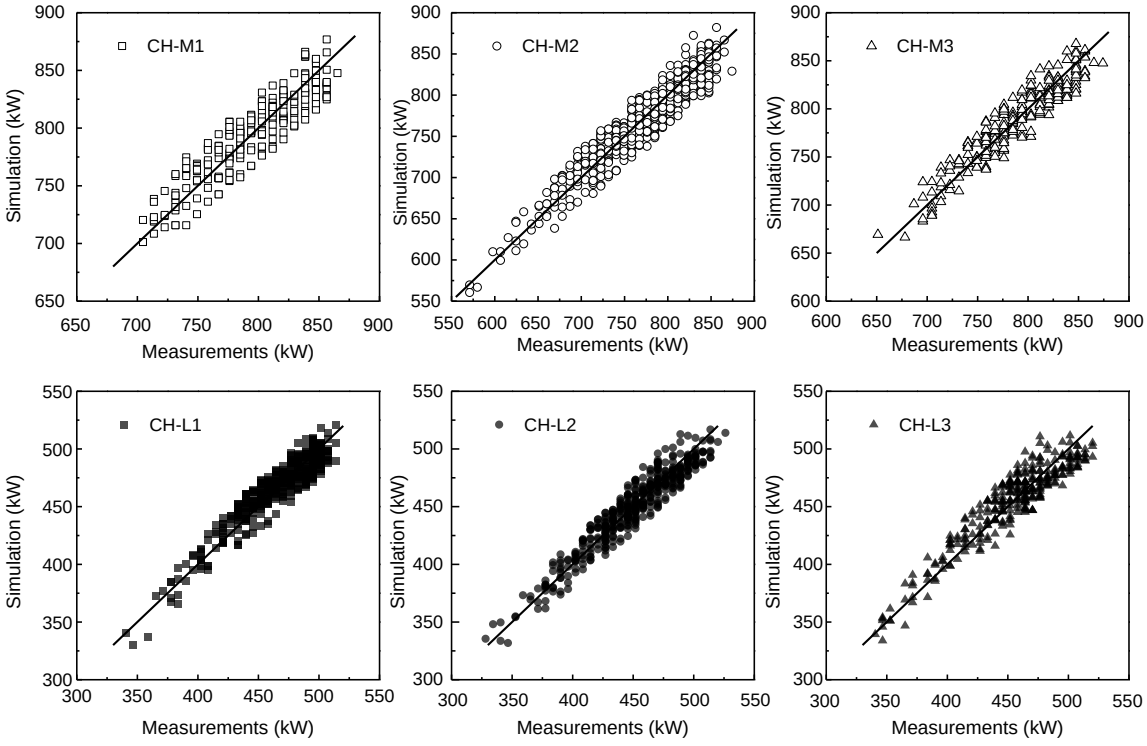

Figure 3: Regression analysis of the chillers' power consumption

Table 1. Coefficients of the chillers' performance curves

Chiller	a_i	b_i	c_i	d_i	e_i	f_i	R^2	Capacity(kW)
CH-M1	-135.398	1127.863	-0.54153	-96.9652	0.31216	0.231704	0.84	4572
CH-M2	-1930.3985	4060.1077	28.4513	-775.3910	-86.4837	1.60808	0.89	4572
CH-M3	944.2316	-1262.45	-30.9648	1015.87	30.3983	0.4991	0.90	4572
CH-L1	-499.355	1412.871	26.4963	-683.551	-6.88704	-0.29631	0.88	2286
CH-L2	-167.361	500.2805	19.8987	111.4599	-4.52549	-0.21494	0.92	2286
CH-L3	-43.7976	1086.149	5.18457	-682.603	2.32859	-0.06421	0.86	2286

3.2 Performance of the control strategies on typical days

3.2.1 Selected typical days

To evaluate the performance of the proposed strategies, two typical days were selected according to the cooling load profile. The two typical days are Aug. 2 and Jun. 15, referred to as a hot summer day and a moderate day, respectively. Figure 4(a) and (b) present the weather conditions and total cooling load profiles on the selected days. On the hot summer day, the wet-bulb temperature ranged from 23.3 °C to 26.9 °C, and the system cooling load ranged from 11648 kW to 16077 kW. On the moderate day, the wet-bulb temperature of the outdoor air was in the range of 21.2 °C to 22.5 °C, and the cooling load ranged from 9480 kW to 10729 kW, which is significantly lower than on the hot summer day. Throughout both days, the cooling load was relatively large, as the cleanrooms operated 24 hours per day.

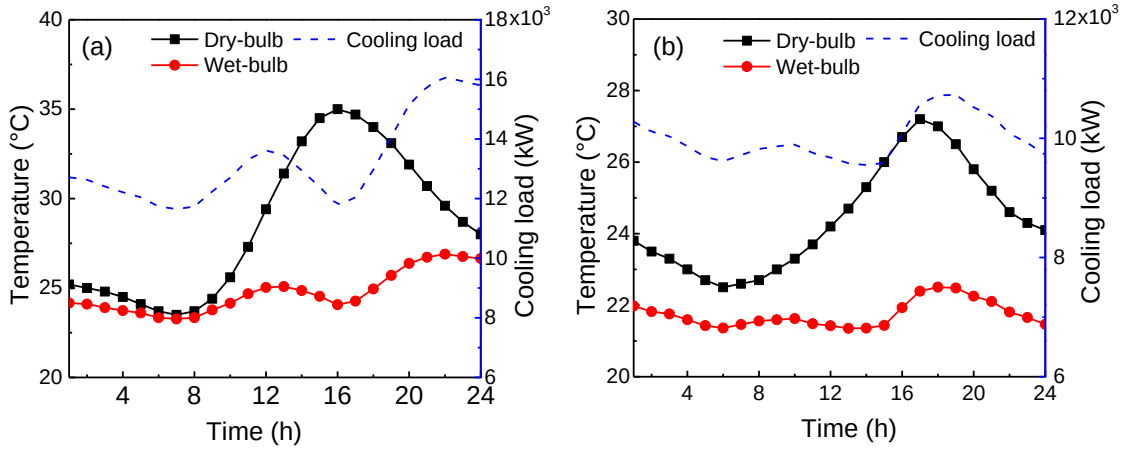

Figure 4: Weather conditions and cooling load profiles on selected days: (a) hot day and (b) moderate day

3.2.2 Hot summer day

Figure 5 shows the hourly allocation of cooling load among chillers under different strategies for a hot summer day. Under strategy A, the cooling loads of the chillers were equal within each chiller group. Using strategy B, the cooling loads of the medium- and low-temperature chiller groups were the same as under strategy A. In each group, the chillers' cooling loads were optimized, and chillers with higher energy efficiency were given priority for use; thus, a larger cooling load was allocated to these chillers. Chiller CH-M2 operated in nearly a full-load condition on the hot summer day, and CH-M3 operated at around 70% of its rated cooling capacity under strategy B, because these chillers exhibited higher energy efficiency than that of CH-M1. Chiller CH-M1 was turned on during the high cooling load periods, 11:00-14:00 and 18:00-00:00.

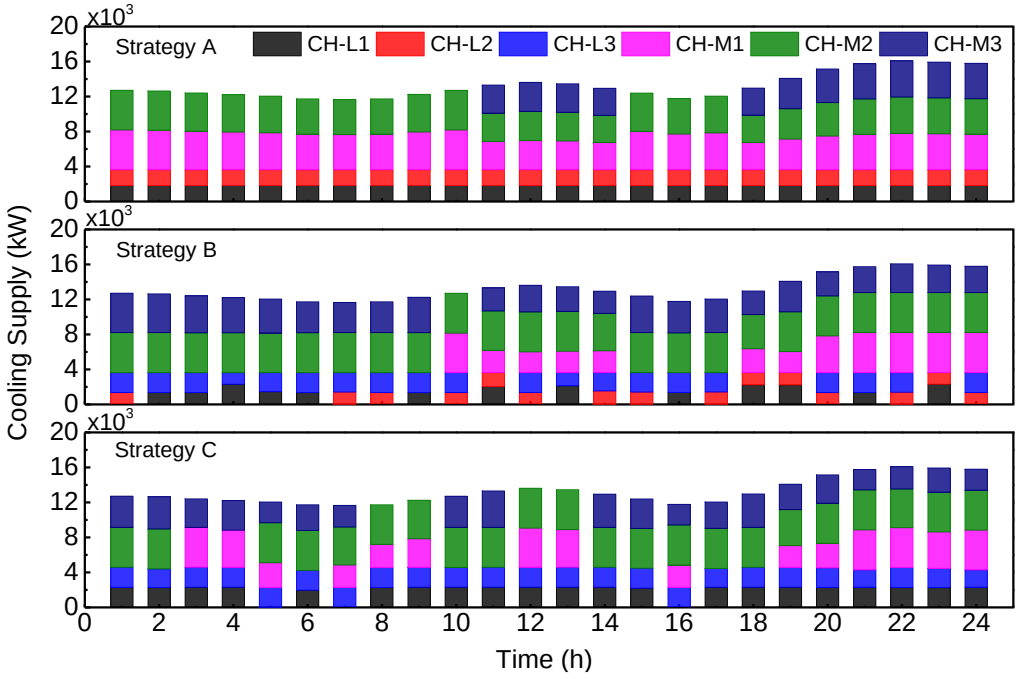

Figure 5: Hourly cooling load distribution of chillers under different strategies

for the hot summer day

Under strategy C, the cooling load distribution between two chiller groups was also optimized by adjusting the temperature of the air leaving the primary cooling coils. For further analysis, the cooling load of each chiller group and the temperature setpoint of the air leaving the primary cooling coils are shown in Figure 6. With identical leaving-air temperature, the cooling supply from each chiller group is the same as under strategies A and B. Under strategy C, the leaving-air temperature setpoint and the cooling supply to the low-temperature chillers were slightly higher than the design conditions on the selected hot summer day. This is because the cooling load of the primary cooling coils was close to or even exceeded the rated capacity of the medium-temperature chillers. Thus, the low-temperature chillers provided more cooling energy (13.9%). In this figure, we can also see that the outlet air temperature setpoint in the periods of 5:00–7:00 and 16:00-17:00 was much lower. This is because the lower bound of the leaving air temperature setpoint declined with the decrease in the inlet air wet-bulb temperature, according to Equation (27). The low outdoor wet-bulb temperature in this period enables the user to reduce the leaving-air temperature setpoint and then reduce the cooling load of low-temperature chillers. As shown in Figure 5, one of the low-temperature chillers was turned off to minimize the energy consumption of the dual-temperature chiller plant during these periods.

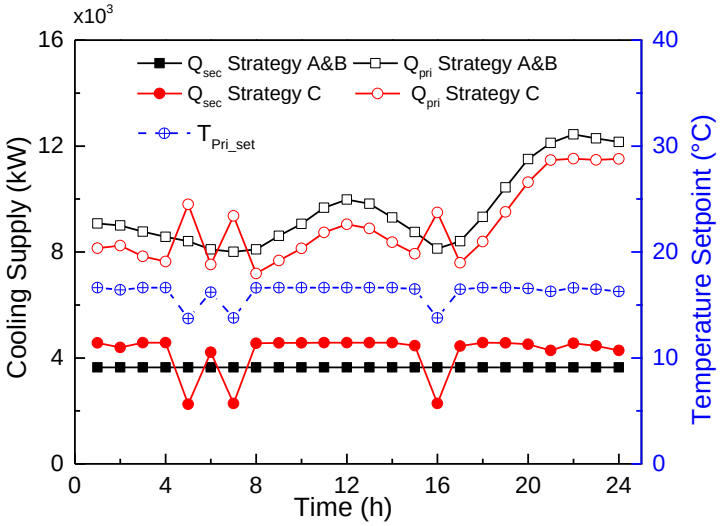

Figure 6: The cooling load of each chiller group and the leaving-air temperature setpoint on the hot summer day

Figure 7 shows the energy consumption and energy savings at each hour for the hot summer day under different strategies. Compared with strategy A, strategy B can reduce the system's energy consumption significantly by optimizing the cooling load of the chillers in each chiller group. The energy reduction under strategy B was 6160 kWh on the hot summer day, which accounts for 7.4% of the total energy consumption. Compared with strategy B, strategy C increased the energy savings by 57.4% by optimizing the cooling load allocation between the two chiller groups. In total, the daily energy reduction under strategy C was 9699 kWh, accounting for 11.6% of the whole plant energy consumption.

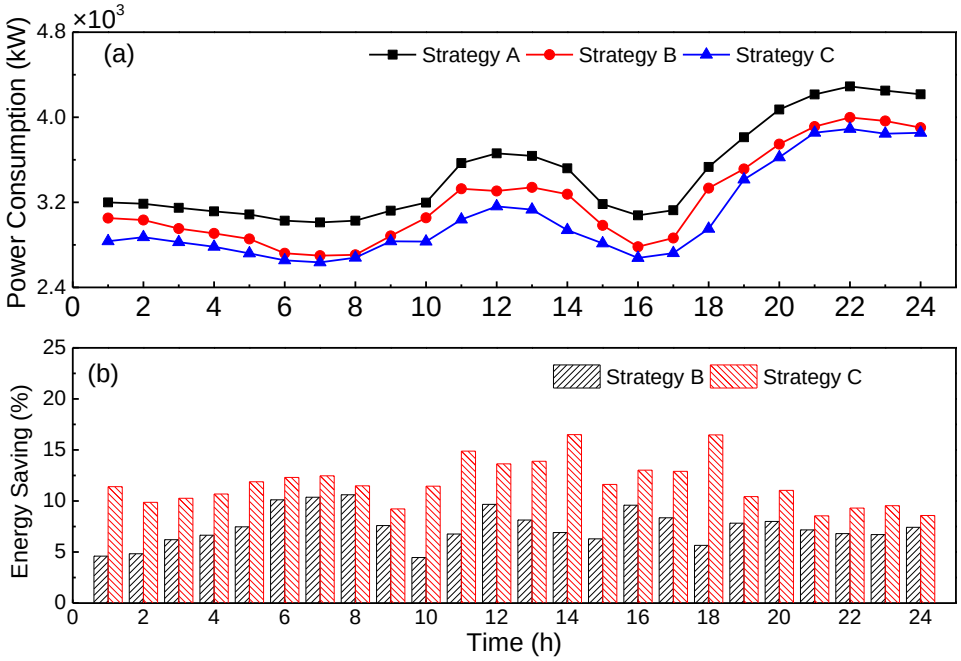

Figure 7: Power consumption and energy-saving rate under different strategies on the hot summer day

3.2.3 Moderate day

Figure 8 depicts the hourly cooling distribution under different control strategies on the moderate day. Similarly, chillers with higher energy efficiency at the corresponding cooling load were used under both optimal control strategies. Under strategy B, CH-L3 operated at nearly the full-load condition, as this chiller exhibited higher energy efficiency at the full-load condition. Under strategy C, the cooling load of low-temperature chiller group was reduced, and only CH-L3 was in operation under nearly the full-load condition at each hour, as a result of the lower outdoor wet-bulb temperature and the temperature of the air leaving the primary cooling coils, as shown in Figure 9. For the medium-temperature chiller group, CH-M2 operated at nearly 100% of its rated capacity at each hour,

and CH-M3 bore the remainder of the cooling load, with an average partial load ratio of 65%.

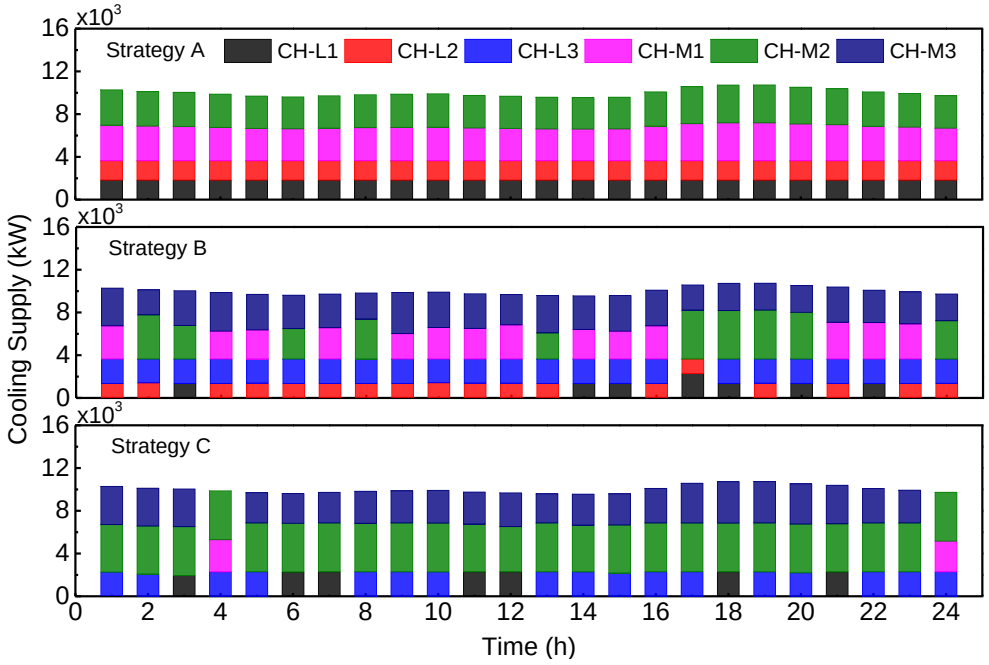

Figure 8: The cooling load of chillers under different control strategies on the moderate day

Figure 9 shows the cooling load of each chiller group and the temperature of the air leaving the primary cooling coils under strategy C. It can be seen that the leaving-air temperature was lower than the constant setpoint of 15.5°, due to the relatively low outdoor wet-bulb temperature. The cooling load of the low-temperature chiller group was reduced by 38.5%, and the cooling load of the medium-temperature chiller groups was increased correspondingly. This is because medium-temperature chillers with higher evaporation temperature normally exhibit higher energy efficiency than low-temperature chillers.

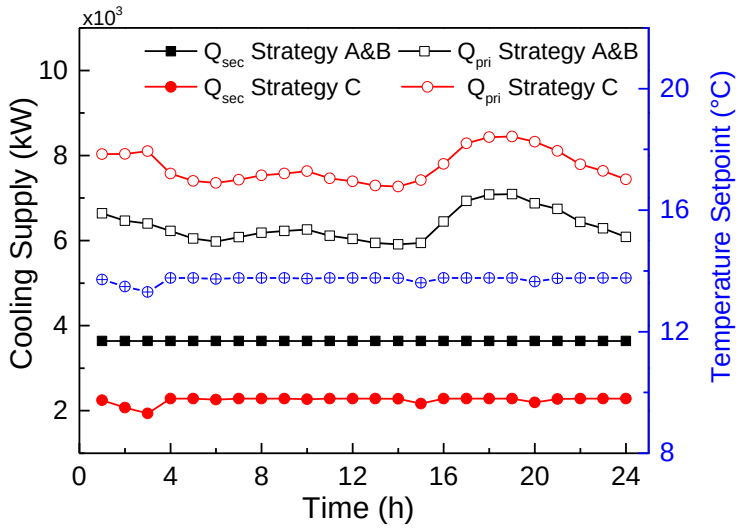

Figure 9: The cooling load of each chiller group and the air temperature setpoint under different strategies on the moderate day

Figure 10 shows the power consumption and energy-saving rate under different strategies on the moderate day. Since the outdoor air wet-bulb temperature was not as high as that on the hot summer day, the total energy consumption of the plant was lower, at 65527 kWh under strategy A. Under strategy B, the total energy reduction was 6442 kWh on the moderate day, which is similar to that on the hot summer day. As the total energy consumption on the moderate day was smaller than that on the hot summer day, the energy-saving rate was greater, accounting for 10.2% of the total energy consumption. Compared with strategy B, the energy reduction under strategy C was 2 times greater, as a result of optimizing the cooling load allocation between two chiller groups. The energy reduction on this moderate day was 1.3 times greater than that on the hot summer day, and it accounted for 20.0% of the total energy consumption

on the moderate day. The large energy savings resulted from the lower leaving-air temperature setpoint, as shown in Figure 9.

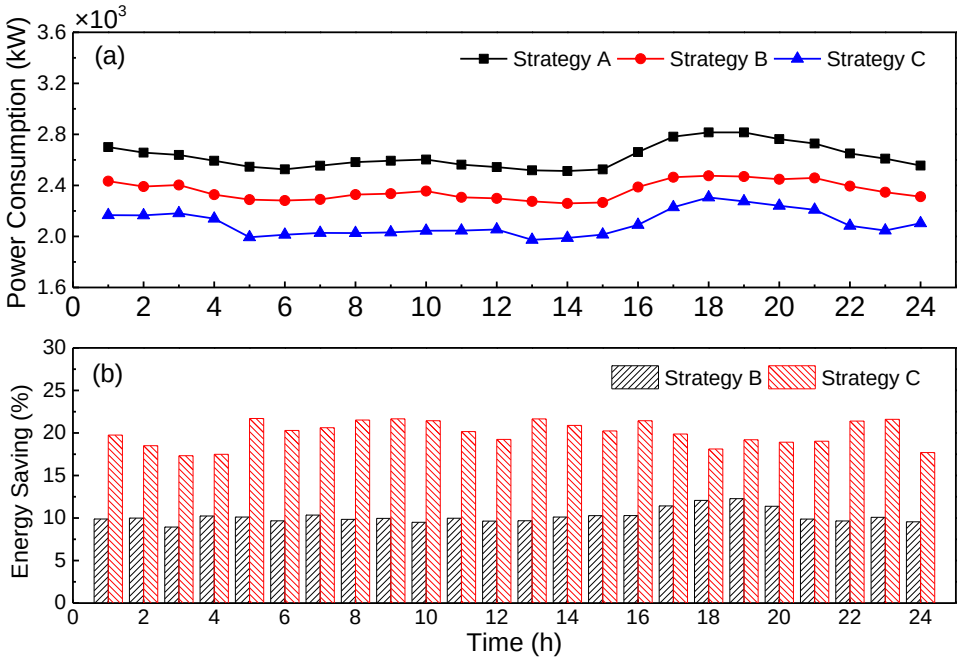

Figure 10: The power consumption and energy-saving rate of different strategies on the moderate day

3.3 Performance throughout the entire cooling season

In a dual-temperature chilled water system, the primary and secondary cooling coils are used together to remove the sensible and latent cooling load of the fresh air.The proposed strategies were applied to the system during the cooling season from May 15 to Sep. 15.

Figure 11 shows the mean energy consumption of the dual-temperature chilled water system for each month, as well as the outdoor wet-bulb temperature. With the increase in the outdoor air wet-bulb temperature, the energy consumption of the system increased from May to July. The system energy consumption

reached its peak value of 2562 kWh in July. From July to September, the energy consumption declined as the system cooling load decreased. Compared with strategy A, strategy B reduced the chillers' energy consumption by optimizing the cooling load of each chiller in the medium- and low-temperature chiller groups separately. The hourly energy savings ranged from 205 kWh to 276 kWh in the cooling season, accounting for 9.3% to 13.5% of the hourly energy consumption. Meanwhile, strategy C further reduced the system energy consumption by regulating the dry bulb temperature of the air leaving the primary cooling coils. The hourly energy savings ranged from 367 kWh to 420 kWh under strategy C. For the entire cooling season, strategy B yielded an estimated energy saving of 651978 kWh, and strategy C was estimated to save about 1053164 kWh in total.

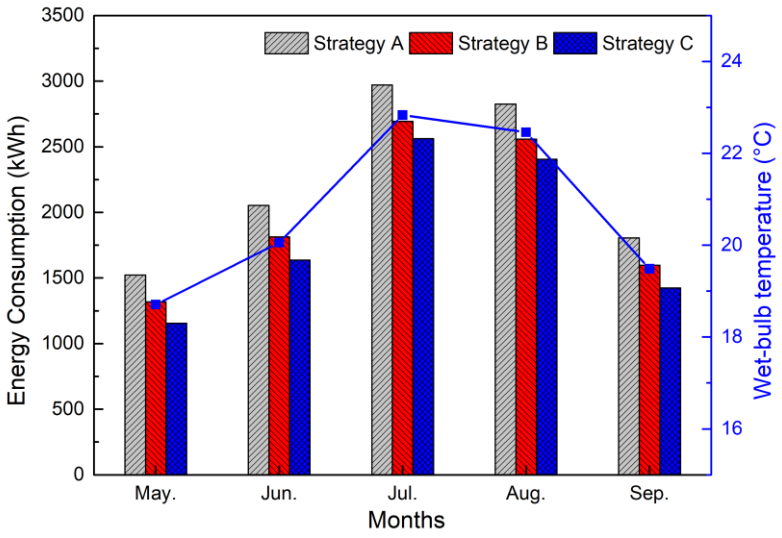

Figure 11 Energy consumption of different strategies during cooling months

The energy-saving rate of the proposed strategy is displayed in Figure 12. Compared with strategy A, strategy B achieved an average energy reduction of 10.1% for the entire cooling season, and the maximum energy saving rate of 13.5% was achieved at the start of the cooling season (May). During the hot summer month of July, the energy-saving rate was slightly lower, around 9.3%. Meanwhile, strategy C further increased the mean energy-saving rate to 16.4% for the entire cooling season, and this rate ranged from 13.8% to 24.1% in different months. Both strategies yielded greater energy savings in moderate months than in hot summer months, since the cooling load was increased significantly in the latter months.

Figure 12 also shows the monthly air temperature leaving the primary cooling coils. Under strategy C, the leaving-air setpoint was lower than that under strategy B, which indicates that strategy C allocated a higher cooling load to the medium-temperature chiller group. In July and August, the leaving-air temperature under strategy C was slightly lower than that under strategy B, indicating a lower cooling load on the low-temperature chiller group. Compared with strategy B, the energy savings of strategy C in July and August were increased by 48.0% and 57.1%, respectively, as medium-temperature chillers normally exhibit higher energy efficiency than low-temperature chillers. In other months, strategy C further increased the energy savings by 73.4% to 82.8%,

as a result of the lower temperature of the air leaving the primary cooling coil. This occurred because the lower bound of the leaving-air temperature decreased with the outdoor wet-bub temperature, which enlarged the energy-saving potential of strategy C. In the hot summer months (July and August), optimization of the cooling load distribution in each chiller group accounted for 63–68% of the total energy savings. In the moderate months, optimizing the cooling load both among chillers within the same group and between two chiller groups accounted for nearly the same proportion of the total energy savings, around 50%. This was because the low outdoor wet-bulb temperature, as well as the cooling load, provided greater control flexibility for the dual-temperature chiller plant.

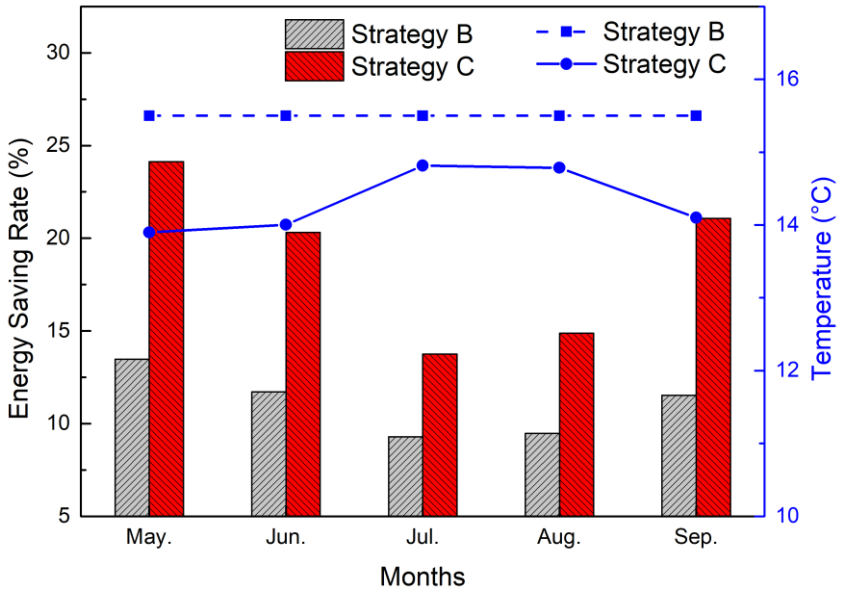

Figure 12 Energy-saving rate of different strategies in the cooling season

4. Discussion

In this study, two optimal control strategies for dual-temperature chilled water

plants were proposed to reduce the total energy consumption of chillers. According to the results, the proposed strategies provide significant energy savings. Since chillers account for a large proportion of the whole cooling system energy consumption, the objective of the optimization was to reduce the energy consumption of chillers without considering the energy consumption of other equipment. When the cooling load distribution between medium- and low-temperature chiller groups changes, the energy consumption of the secondary pumps changes correspondingly, but the secondary pumps' energy consumption accounts for only a small proportion of the total energy consumption of the whole plant. In addition, when the cooling load is redistributed between two chiller groups, the energy consumption of one group of secondary pumps increases, while it decreases for the other group. Thus, the total energy consumption change of secondary pumps has little effect on the overall energy consumption, and it was not considered in the current study. In the future, holistic optimization that addresses the synergistic effects of multiple variables to maximize the energy efficiency of the dual-temperature central cooling system will be studied, considering the energy consumption of chillers as well as all other auxiliary equipment, such as chilled water pumps, cooling water pumps and cooling towers.

Furthermore, the optimization in this study considered only the single objective of reducing the system energy consumption. The output varies with the outdoor

weather conditions and cooling load, while the fluctuation of the control variables may be significant, such as the air temperature setpoint on a hot summer day between 4:00 and 8:00. Therefore, in a future study, the optimization process should considere the fluctuation of the setpoints among adjacent time steps in order to avoid unstable operation, by conducting multi-objective optimization or by adding constraints to the optimization.

5. Conclusions

This study proposed two optimal chiller loading strategies for dual-temperature chilled water plants. Strategy B optimizes the cooling load distribution among the chillers in each group by adjusting the partial load of each chiller, which is similar to the method for a single-temperature chiller plant. Strategy C optimizes the cooling load between two chiller groups by regulating the temperature of the air leaving the primary cooling coils and the cooling load of each chiller simultaneously. The proposed optimal control strategies were applied to a dual-temperature chilled water plant serving MAUs in a semiconductor factory throughout the entire cooling season. The results suggest that both strategies result in significant energy savings, with an average energy reduction of 10.1% for the entire cooling season under strategy B and 16.4% under strategy C. Meanwhile, strategy C achieved higher energy savings than strategy B, because the former strategy considered the cooling load distribution both among chillers in the same group and between two chiller groups. In the hot

summer months, optimizing the cooling load distribution among chillers in each chiller group was the dominant measure, as it accounted for 63-68% of the total energy savings. In the moderate months, both optimizing the cooling load distribution among chillers in the same group and optimizing the distribution between two chiller groups are essential measures, as they accounted for nearly the same proportion of the total energy savings.

In a real chiller plant, the proposed strategy can be implemented by converting the partial load ratio of each chiller to the chilled water supply temperature according to Equation (11) and resetting the temperature of the air leaving the primary cooling coils. These strategies can also be used as references by operators as they regulate the setpoints of chillers.

Acknowledgements

This work was supported by the China National Key Research and Development Program [Grant No. 2018YFC0705203]; the Tianjin Science and Technology Commission [Grant No.18ZXAQSF00070]; and the China Scholarship Council [No. 201806250235].

References

[1] Yang, L., Yan, H. and Lam, J.C. Thermal comfort and building energy consumption implications – A review. Applied Energy, 2014. 115: p. 164-173.

[2] Abergel, T., Delmastro, C. and Lane, K. Tracking Buildings 2019.

https://www.iea.org/reports/tracking-buildings.

[3] Li, D.H.W., Yang, L. and Lam, J.C. Zero energy buildings and sustainable development implications – A review. Energy, 2013. 54: p. 1-10.

[4] Clift, R. Climate change and energy policy: The importance of sustainability arguments. Energy, 2007. 32(4): p. 262-268.

[5] Pérez-Lombard, L., Ortiz, J. and Pout, C. A review on buildings energy consumption information. Energy and Buildings, 2008. 40(3): p. 394-398.

[6] Ali, M., et al. Energy analysis of chilled water system configurations using simulation-based optimization. Energy and Buildings, 2013. 59: p. 111-122.

[7] Wang, S. Intelligent Buildings and Building Automation. 2010: Spon Press.

[8] Zhang, T., Liu, X. and Jiang, Y. Development of temperature and humidity independent control (THIC) air-conditioning systems in China—A review. Renewable and Sustainable Energy Reviews, 2014. 29: p. 793-803.

[9] Tsao, J., et al. Saving energy in the make-up air unit (MAU) for semiconductor clean rooms in subtropical areas. Energy and Buildings, 2008. 40(8): p. 1387-1393.

[10] Nall, D.H. Dual Temperature Chilled Water Plant & Energy Savings. ASHRAE Journal, 2017. 59(6): p. 70.

[11] Liao, Y., et al. Uncertainty analysis for chiller sequencing control. Energy and Buildings, 2014. 85: p. 187-198.

[12] Shan, K., et al. Development and validation of an effective and robust

chiller sequence control strategy using data-driven models. Automation in Construction, 2016. 65: p. 78-85.

[13] Huang, S., Zuo, W. and Sohn, M.D. Amelioration of the cooling load based chiller sequencing control. Applied Energy, 2016. 168: p. 204-215.

[14] Liu, Z., et al. Optimal chiller sequencing control in an office building considering the variation of chiller maximum cooling capacity. Energy and Buildings, 2017. 140: p. 430-442.

[15] Ahn, K.U., et al. Optimal control strategies of eight parallel heat pumps using Gaussian process emulator. Journal of building performance simulation, 2019. 12(5): p. 650-662.

[16] Li, Z., Huang, G. and Sun, Y. Stochastic chiller sequencing control. Energy and Buildings, 2014. 84: p. 203-213.

[17] Liao, Y., et al. Robustness analysis and enhancement of chiller sequencing control under uncertainties. Procedia Engineering, 2017. 205: p. 1878-1885.

[18] Liao, Y. and Huang, G. A hybrid predictive sequencing control for multi-chiller plant with considerations of indoor environment control, energy conservation and economical operation cost. Sustainable Cities and Society, 2019. 49: p. 101616.

[19] ASHRAE. ASHRAE Handbook-HVAC Application (SI). American Society of Heating, Refrigerating and Air-Conditioning Engineers, Inc., Atlanta,

USA, 2011.

[20] Chen, Y., et al. Design and operation optimization of multi-chiller plants based on energy performance simulation. Energy and Buildings, 2020. 222: p. 110100.

[21] Abou-Ziyan, H.Z. and Alajmi, A.F. Effect of load-sharing operation strategy on the aggregate performance of existed multiple-chiller systems. Applied Energy, 2014. 135: p. 329-338.

[22] Chang, Y. and Tu, H. An effective method for reducing power consumption optimal chiller load distribution. in International Conference on Power System Technology. 2002: IEEE.

[23] Chang, Y. A novel energy conservation method—optimal chiller loading. Electric Power Systems Research, 2004. 69(2-3): p. 221-226.

[24] Chang, Y. Genetic algorithm based optimal chiller loading for energy conservation. Applied Thermal Engineering, 2005. 25(17-18): p. 2800-2815.

[25] Chang, Y., Lin, J. and Chuang, M. Optimal chiller loading by genetic algorithm for reducing energy consumption. Energy and Buildings, 2005. 37(2): p. 147-155.

[26] Chang, Y., Lin, F. and Lin, C.H. Optimal chiller sequencing by branch and bound method for saving energy. Energy Conversion and Management, 2005. 46(13-14): p. 2158-2172.

[27] Chang, Y. An innovative approach for demand side management—optimal chiller loading by simulated annealing. Energy, 2006. 31(12): p. 1883-1896.

[28] Chang, Y. Optimal chiller loading by evolution strategy for saving energy. Energy and Buildings, 2007. 39(4): p. 437-444.

[29] Lee, W. and Lin, L. Optimal chiller loading by particle swarm algorithm for reducing energy consumption. Applied Thermal Engineering, 2009. 29(8-9): p. 1730-1734.

[30] Ardakani, A.J., Ardakani, F.F. and Hosseinian, S.H. A novel approach for optimal chiller loading using particle swarm optimization. Energy and Buildings, 2008. 40(12): p. 2177-2187.

[31] Coelho, L.D.S. and Mariani, V.C. Improved firefly algorithm approach applied to chiller loading for energy conservation. Energy and Buildings, 2013. 59: p. 273-278.

[32] Coelho, L.D.S., et al. Optimal chiller loading for energy conservation using a new differential cuckoo search approach. Energy, 2014. 75: p. 237-243.

[33] Lo, C., Tsai, S. and Lin, B. Economic dispatch of chiller plant by improved ripple bee swarm optimization algorithm for saving energy. Applied Thermal Engineering, 2016. 100: p. 1140-1148.

[34] Zheng, Z. and Li, J. Optimal chiller loading by improved invasive weed optimization algorithm for reducing energy consumption. Energy and Buildings, 2018. 161: p. 80-88.

[35] Sohrabi, F., et al. Optimal chiller loading for saving energy by exchange market algorithm. Energy and Buildings, 2018. 169: p. 245-253.

[36] Lin, C., et al. Applying two-stage differential evolution for energy saving in optimal chiller loading. Energies, 2019. 12(4): p. 622.

[37] Zheng, Z., Li, J. and Duan, P. Optimal chiller loading by improved artificial fish swarm algorithm for energy saving. Mathematics and Computers in Simulation, 2019. 155: p. 227-243.

[38] Teimourzadeh, H., Jabari, F. and Mohammadi-ivatloo, B. An augmented group search optimization algorithm for optimal cooling-load dispatch in multi-chiller plants. Computers & Electrical Engineering, 2019: p. 106434.

[39] Askarzadeh, A. and Coelho, L.D.S. Using two improved particle swarm optimization variants for optimization of daily electrical power consumption in multi-chiller systems. Applied Thermal Engineering, 2015. 89: p. 640-646.

[40] Beghi, A., Cecchinato, L. and Rampazzo, M. A multi-phase genetic algorithm for the efficient management of multi-chiller systems. Energy Conversion and Management, 2011. 52(3): p. 1650-1661.

[41] Beghi, A., et al. A PSO-based algorithm for optimal multiple chiller systems operation. Applied Thermal Engineering, 2012. 32: p. 31-40.

[42] Chen, C., Chang, Y. and Chan, T. Applying smart models for energy saving in optimal chiller loading. Energy and Buildings, 2014. 68: p. 364-371.

[43] Chan, T., Chang, Y. and Huang, J. Application of artificial neural network and genetic algorithm to the optimization of load distribution for a multiple-type-chiller plant. Building Simulation, 2017. 10(5): p. 711-722.

[44] Yang, X. Nature-Inspired Optimization Algorithms, ed. X. Yang. 2014, Oxford: Elsevier.

[45] ASHRAE. ASHRAE HANDBOOK Heating, Vetilation, and Air-Conditioning system and equipment. 2016.

[46] Wang, Y., et al. A simplified modeling of cooling coils for control and optimization of HVAC systems. Energy Conversion and Management, 2004. 45(18-19): p. 2915-2930.